Supplemental Figure Legends

Figure S1. Psoralen and AP-ICLs are Unhooked in a Replication-Dependent Manner, Related to Figure 1

(A) Model of replication-coupled cisplatin-ICL repair. See main text for details.

(B) Extent of cross-linking for pICLs. ICL-containing plasmids were digested with NotI and the resulting fragments were 5' end radiolabeled, separated on a denaturing polyacrylamide gel, and visualized by autoradiography. The fraction of plasmid in the cross-linked band versus the ssDNA band plus the cross-linked band was calculated and in each case was found to be at least 97%. For pICL-*lacO*^{Pso}, there was an additional, faster migrating band (*) that likely represents cross-linked species that was not denatured during electrophoresis.

(C) Unhooking assay for pICL^{Pso} and pICL^{AP}. Digestion of pICL^{Pso} and pICL^{AP} generates an X-structure prior to unhooking and linear species subsequent to unhooking.

(D) Replication-dependent unhooking of pICL^{Pso} and pICL^{AP}. pICL^{Pso} and pICL^{AP} were replicated in egg extract in the presence or absence of geminin, as indicated. Repair intermediates were digested with HincII, separated on a denaturing agarose gel, and visualized by Southern blotting. Generation of the unhooked linear species illustrated in (C) was blocked in the absence of DNA replication.

(E) Error-free repair assay for pICL^{Pso}. pICL^{Pso} contains an NheI site that is blocked by the ICL but becomes cleavable after error free repair. Digestion of repaired plasmids with HincII and NheI generates 3.6 kb and 2.0 kb fragments.

(F) Error-free repair of pICL^{Pso}. pICL^{Pso} was replicated in egg extract in the presence or absence of geminin, as indicated. Repair intermediates were digested with HincII or HincII and NheI, separated on a native agarose gel, and visualized by Southern blotting. A 1.2 kb ApaLI-digested pCtrl fragment was added before DNA extraction as a loading control. 33% of input pCtrl was digested with HincII/Nhe1 and loaded in lane 13.

(G) Quantification of error-free repair efficiency of pICL^{Pso} shown in (F). Efficiency of error-free pICL^{Pso} repair was quantified as the ratio of error-free repair products to total linear species ([3.6 kb + 2.0 kb]/[5.6 kb +3.6 kb + 2.0 kb]).

(H) FANCI-D2 immunodepletion. Mock-depleted and FANCI-D2-depleted NPE was analyzed by Western blotting using FANCI or FANCD2 antibody. A relative volume of 100 corresponds to 0.25 µl NPE.

(I) pICL^{Pso} stimulates FANCD2 ubiquitylation. pCtrl, pICL^{Pt}, or pICL^{Pso} was replicated in egg extract and, at the indicated times, samples of total extract were analyzed by Western blotting using FANCD2 antibody. Samples shown were processed in parallel but analyzed on separate blots. Replication of pCtrl also caused some basal level of FANCD2 ubiquitylation, consistent with earlier observations (Raschle et al., 2008; Taniguchi et al., 2002).

(J) The 3.6 kb and 2.0 kb fragments in Figure 2H were quantified and plotted.

Figure S2. Repair of a 2'FdT-Psoralen-ICL Requires FANCI-FANCD2, Related to Figure 3

(A) FANCI-D2 immunodepletion. Mock-depleted NPE, FANCI-D2-depleted NPE (ΔI-D2), and ΔI-D2 NPE supplemented with xFANCI-D2 (ΔI-D2+xI-D2) were blotted with FANCI or FANCD2 antibody. A relative volume of 100 corresponds to 0.25 µl NPE.

(B) pICL^{Pt} or pICL$^{FdT-Pso}$ was replicated in mock or FANCI-D2 depleted egg extracts in the presence of [α-^{32}P]dATP and analyzed as in Figure 1C. White arrowheads, Figure 8 structures that persist in the absence of FANCI-D2. The fraction Figure 8 indicates the proportion of Figure 8 structures relative to total species at 300 min.

(C) pICL$^{FdT-Pso}$ was replicated in mock-depleted egg extract, FANCI-D2 depleted extract (ΔI-D2), or ΔI-D2 extract supplemented with xFANCI-D2 (ΔI-D2 + xI-D2) in the presence of [α-^{32}P]dATP (Experiment described in Figure 3C). DNA was purified and digested with AflIII and EcoRI before separation on a denaturing polyacrylamide gel.

Figure S3. Model for repair of a Psoralen-ICL, Related to Figure 3.

Repair of a thymidine-psoralen-ICL (black arrows) or 2' fluoro-thymidine-psoralen-ICL (pink arrows) by incision-independent (left branch) or incision-dependent (right branch) pathways. See main text for details. Black lines, parental DNA. Red lines, nascent leading strands. Cyan, psoralen-ICL. Green ovals, CMG helicase. Closed circles indicate point mutations that arise due to bypass of an AP site. Open circles indicate potential point mutations that may be introduced due to bypass of a thymine monoadduct. Note that although bypass of a guanine monoadduct derived from a cisplatin-ICL was previously shown to be largely error-free, it is unknown whether bypass of a thymine monoadduct derived from a psoralen-ICL is mutagenic.

Figure S4. CMG Unloading is Required for 2'FdT-Psoralen-ICL Repair, Related to Figure 4.

(A) Plasmid pull down assays. pCtrl (containing 48 *lacO* repeats but without damage) was replicated in the presence or absence of the p97 inhibitor NMS-873, and samples were stopped at the indicated times, followed by plasmid pull down using LacI-coated beads. Western blotting was performed on chromatin samples with the indicated antibodies.

(B) pICL was replicated in the presence or absence of NMS-873 with [α-^{32}P]dATP and analyzed as in Figure 1C. The fraction Figure 8 indicates the proportion of Figure 8 structures relative to total species at 180 min.

(C) Samples from (B) were purified and digested with AflIII and EcoRI before separation on a denaturing polyacrylamide gel and visualization by autoradiography.

Figure S5. AP-ICL Repair Requires Replication but not CMG Unloading or FANCI-FANCD2, Related to Figure 5.

(A) Error-free repair of pICL^{AP}. pICL^{AP} was replicated in egg extract in the presence or absence of geminin, as indicated. Repair intermediates were digested with HincII or HincII/SapI, separated on a native agarose gel, and visualized by Southern blotting. A 0.9 kb HindIII-

digested pCtrl fragment was added before DNA extraction as a loading control. 50% of input pCtrl was digested with HincII or HincII/SapI and loaded in lanes 9 and 18, respectively. Digestion of repaired plasmids with HincII/SapI generates 3.3 kb and 2.3 kb fragments.

(B) Quantification of error-free repair efficiency of pICL^{AP} shown in (A). Efficiency of error-free pICL^{AP} repair was quantified as the ratio of error-free repair products to total linear species ([3.3 kb + 2.3 kb]/[5.6 kb +3.3 kb + 2.3 kb]) and graphed.

(C) FANCI-D2 immunodepletion. Mock-depleted and FANCI-D2-depleted NPE was analyzed by Western blotting using FANCI or FANCD2 antibody. A relative volume of 100 corresponds to 0.66 µl NPE.

(D) pICL^{AP} (containing 48 *lacO* repeats) was replicated in the presence or absence of NMS-873 and, at the indicated times, pulled down using LacI-coated beads. Chromatin samples were analyzed by Western blotting with the indicated antibodies.

(E) pICL^{Pt} and pICL^{AP} were replicated with [α-^{32}P]dATP in the presence or absence of NMS-873 and analyzed as in Figure 1C.

(F) pICL^{AP} was replicated in mock-depleted egg extract (ΔMock), FANCI-D2 depleted extract (ΔI-D2), or ΔI-D2 extract supplemented with xFANCI-D2 (ΔI-D2 + xI-D2) in the presence of [α-^{32}P]dATP. DNA was purified and digested with AflIII before separation on a denaturing polyacrylamide gel and visualization by autoradiography. Two portions of the autoradiograph are shown with different contrast for optimal display. White arrowhead, -1 product of the rightward fork that persists in the absence of FANCI-D2.

Figure S6. AP-ICL Unhooking Requires Replication Fork Convergence, Related to Figure 6.

(A) Cartoon of pICL-*lacO*^{AP} containing an array of 48 *lacO* repeats. In order to determine whether AP-ICL repair requires convergence of two replication forks at the ICL (as seen for cisplatin- and psoralen-ICLs; Zhang et al., 2015), we constructed plasmids containing an AP-

ICL adjacent to an array of 48 *lac* repressor binding sites. Binding of LacI to the *lacO* array prevents progression of the leftward replication fork to the ICL

(B) Expected outcomes of pICL-*lacO*^{AP} replication in the presence of buffer, LacI, and LacI + IPTG. In the absence of LacI, two replication forks converge on the ICL. In the presence of LacI, progression of the leftward replication fork is blocked and only the rightward replication fork encounters the ICL. Addition of IPTG releases prevents the block to leftward fork progression and both forks are able to converge on the ICL.

(C) Schematic illustration of nascent leading strands generated in the presence and absence of LacI in the experiments shown in (D) and (E).

(D-E) Nascent strand analysis of pICL-*lacO*^{AP} replication intermediates with the AP site on the top parental strand (D) or bottom parental strand (E), with or without LacI and IPTG, as indicated. pICL-*lacO*^{AP} plasmids were pre-incubated with buffer or LacI and then replicated in egg extract. At the times indicated, the nascent strands were purified, digested with AflIII and EcoRI, separated on a polyacrylamide gel, and visualized by autoradiography. Images were adjusted separately in different panels for optimal display. When the AP site is located on the top strand (and no LacI is present), prominent stalling of the leftward fork is observed (D, lanes 2-4), as in Figure 5F (lanes 14-16) due to a requirement for TLS to bypass the AP site. When the AP site is located on the bottom strand (and no LacI is present), prominent stalling of the rightward fork is seen (E, lanes 2-4). Importantly, when LacI is present to block arrival of the leftward fork, the AP-ICL causes persistent arrest of the rightward leading strand near the -20 position (arrowheads), regardless of whether the rightward leading strand encounters the adenosine-side (D) or the AP-side (E) of the ICL. Stalling at -20 is relieved by addition of IPTG, which causes LacI to dissociate form the *lacO* array and allows the leftward fork to encounter the ICL. This persistence of CMG at the AP-ICL (inferred from the -20 leading strand arrest) after arrival of only a single fork strongly implies that convergence of two replication forks is required to promote *N*-glycosyl bond cleavage.

Figure S7. ICL Repair Requires CMG Unloading in the Absence of NEIL3-Dependent Unhooking, Related to Figure 7.

(A) NEIL3 immunodepletion. Mock-depleted and NEIL3-depleted NPE was analyzed by Western blotting using NEIL3 antibody. A relative volume of 100 corresponds to 0.25 µl NPE.

(B) SDS-PAGE of recombinant NEIL3. Purified WT and K60A-mutated NEIL3 were separated on a 4-20% acrylamide gel and visualed by Coomassie staining.

(C) pCtrl or pICL^{Pt} was replicated in mock-depleted egg extract, NEIL3-depleted egg extract, or NEIL3-depleted egg extract supplemented with recombinant NEIL3 in the presence of [α-^{32}P]dATP and analyzed as in Figure 1C.

(D) pICL^{Pso} or pICL^{AP} was replicated in mock-depleted or NEIL3-depleted egg extract supplemented with [α-^{32}P]dATP in the presence or absence of NMS-873 and analyzed as in Figure 1C. White arrowheads, Figure 8 structures that persist for pICL^{Pso} and pICL^{AP} in the presence of NMS-873 upon NEIL3-depletion. The fraction Figure 8 indicates the proportion of Figure 8 structures relative to total species at 240 min.

(E) 300 nM recombinant NEIL3 was used to rescue NEIL3 depletions in Figures 7A and S7C. However, we subsequently determined that the endogenous NEIL3 concentration is ~ 7 nM (left panel). We therefore repeated the rescue experiment and found that as little as ~ 15 nM recombinant NEIL3 was sufficient to rescue incision-independent unhooking in NEIL3-depleted extract (right panel). While 15 nM still exceeds the endogenous concentration by ~2-fold, this likely reflects the fact that recombinant NEIL3 is generally only partially active (Liu et al., 2012).

Table

Table S1. Oligonucleotide Sequences, Related to STAR Methods

Oligonucleotides for preparation of AP-ICL unhooking substrates

Name	Sequence (cross-linked positions are indicated in bold)	Source
top strand (DNA)	GCCATAGTAAG**A**AGAGCCGAATGC	IDT
top strand (DNA/RNA)	rGrCrCrArUrArGrUrArAG**A**ArGrArGrCrCrGrArArUrGrC	IDT
bottom strand (DNA)	GCATTCGGCTC**dU**TCTTACTATGGC	IDT
bottom strand (DNA/RNA)	rGrCrArUrUrCrGrGrCrUC**dU**TrCrUrUrArCrUrArUrGrGrC	IDT

Oligonucleotides for preparation of pICLs

Name	Sequence (cross-linked positions are indicated in bold)	Source
Psoralen ICL (top stand)	CCCCGGGGC**T**AGCC	IDT
Psoralen ICL (bottom stand)	GCACGGC**T**AGCCCC	IDT
2'FdT Psoralen ICL (top stand)	CCCCGGGGC(**2'FdT)**AGCC	Keck Foundation Biotechnology Resource Laboratory at Yale University
2'FdT Psoralen ICL (bottom stand)	GCACGGC(**2'FdT**)AGCCCC	Keck Foundation Biotechnology Resource Laboratory at Yale University
AP ICL (top strand)	CCCTCTTCCGCTC**dU**TCTTTC	IDT
AP ICL (bottom strand)	GCACGAAAG**A**AGAGCGGAAG	IDT
reverse orientation AP ICL (top strand)	CCCTGAAAG**A**AGAGCGGAAG	IDT
reverse orientation AP ICL (bottom strand)	GCACCTTCCGCTC**dU**TCTTTC	IDT

Oligonucleotide primers for preparation of pFastBac1-NEIL3-FLAG and pFastBac1-NEIL3-K60A-FLAG

Name	Sequence	Source
Primer A	CAATTATGGTGGAGGGTCCGGG	IDT
Primer B	CTGTTTCACGTCTACTCTGTTTTTGCCC	IDT
Primer C	GCGCGCGGAATTCACCATGGTGGAGGGTCCGGGCTG	IDT
Primer D	CCAGCCCTCGAGCGTCTACTTGTCGTCATCGTCTTTGTAGTCACATGCCCAGTG(	IDT
Primer E	GCTACGCTGGAGTGGAAACGCTGGGAGCGGAGCTTTTTATAT	IDT
Primer F	ATATAAAAAGCTCCGCTCCCAGCGTTTCCACTCCAGCGTAGC	IDT

Sequencing ladder primer	CATGTTTTACTAGCCAGATTTTTCCTCCTCTCCTG	Operon

Figure S1

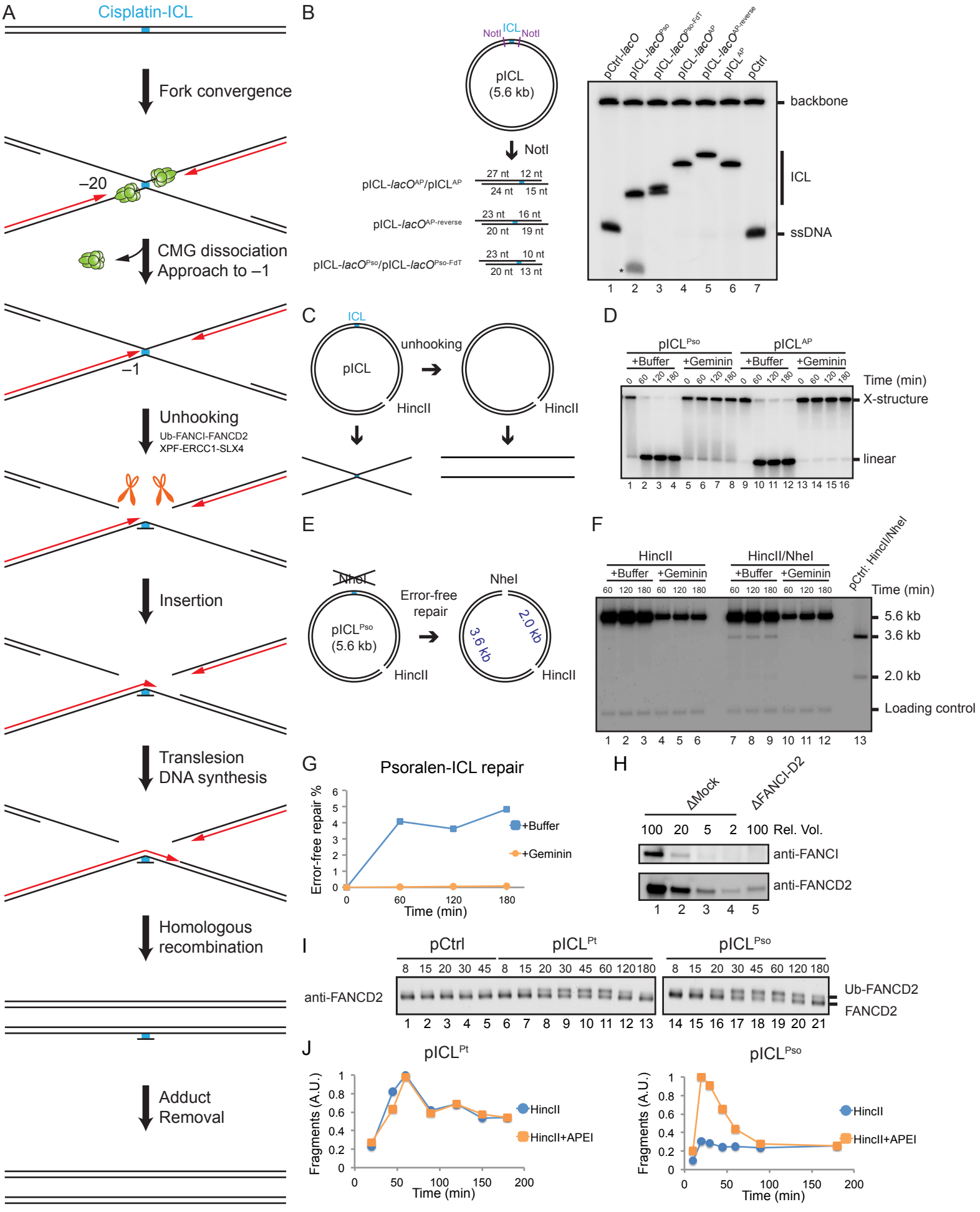

Figure S2

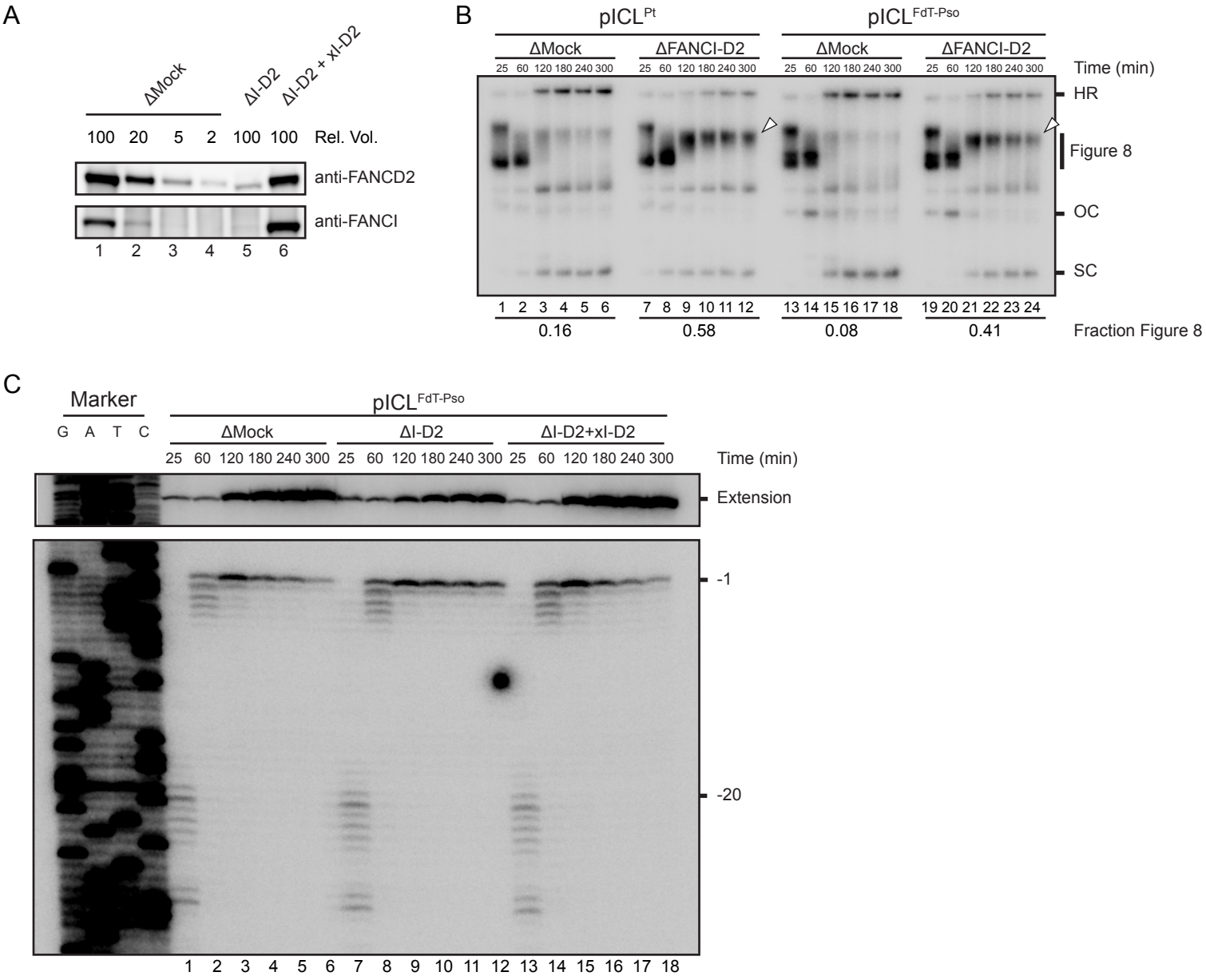

Figure S3

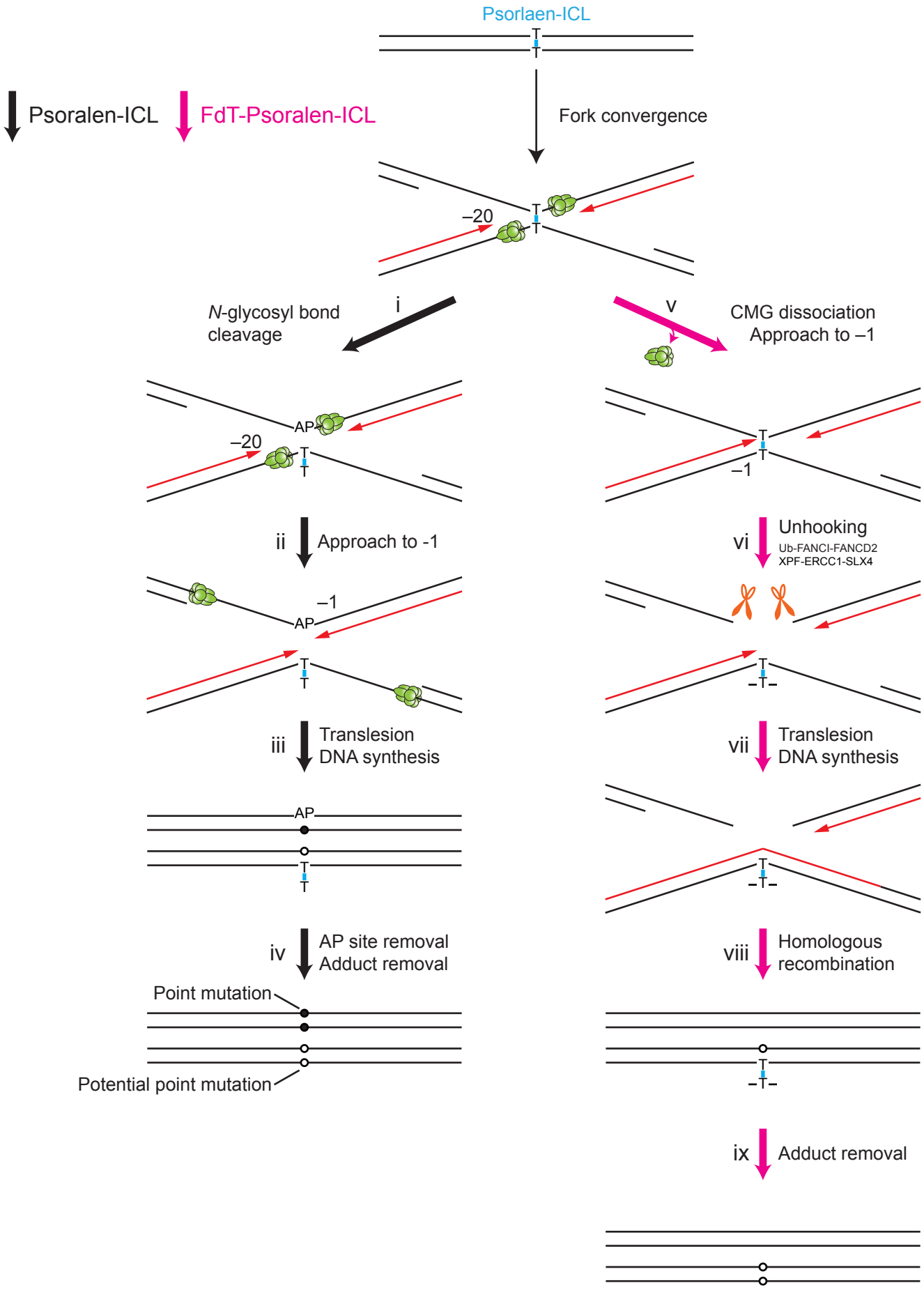

Figure S4

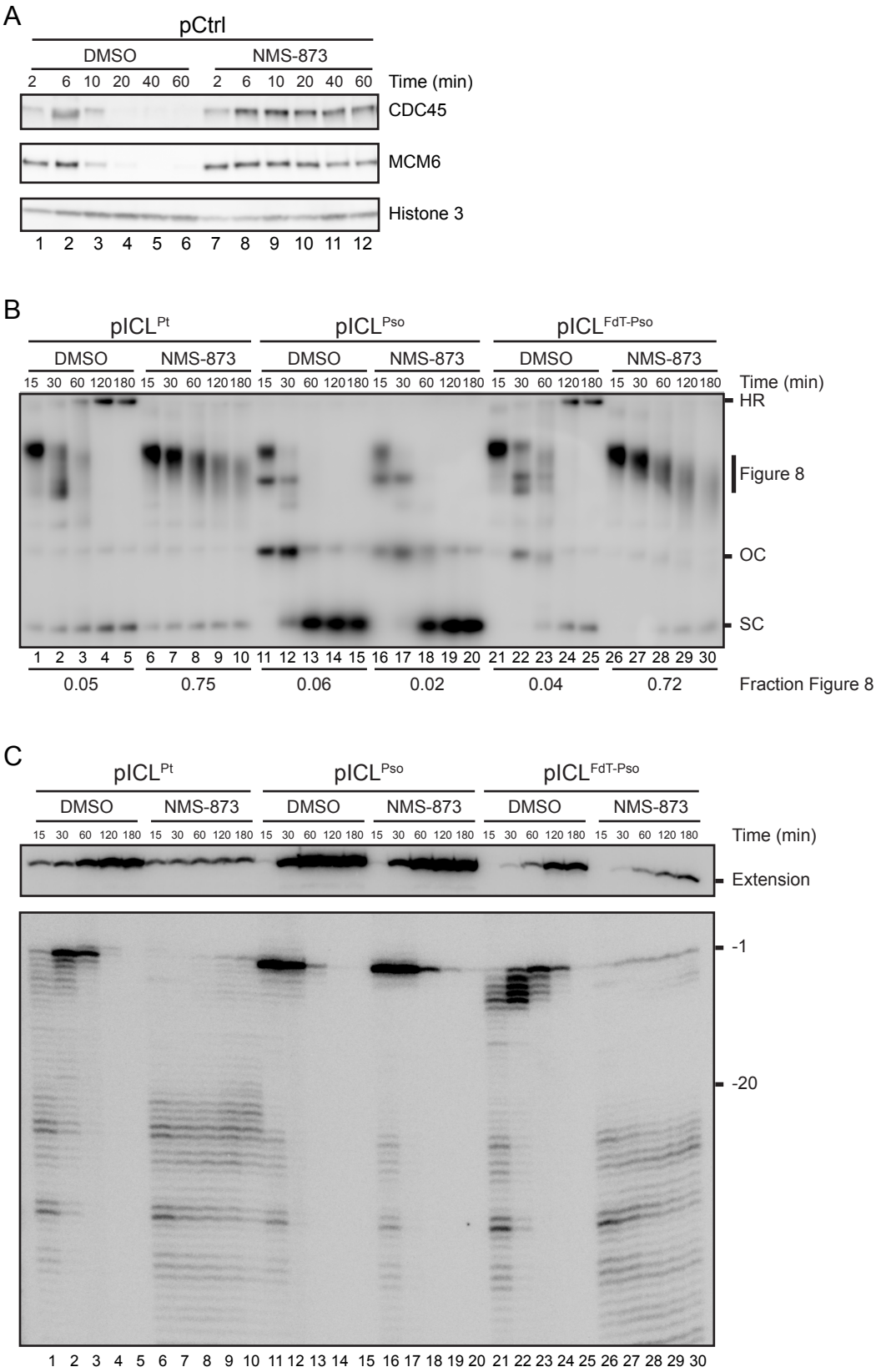

Figure S5

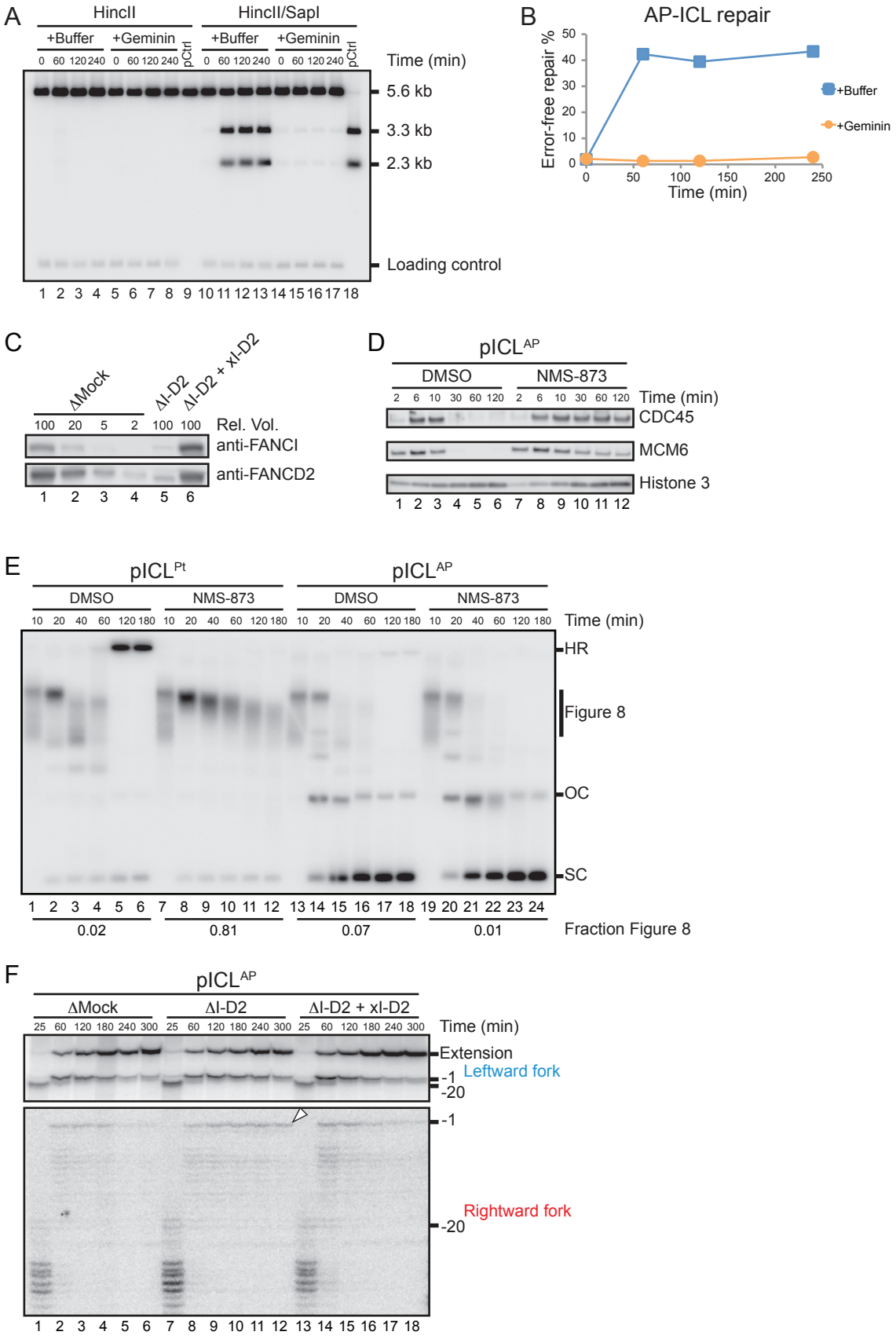

FIgure S6

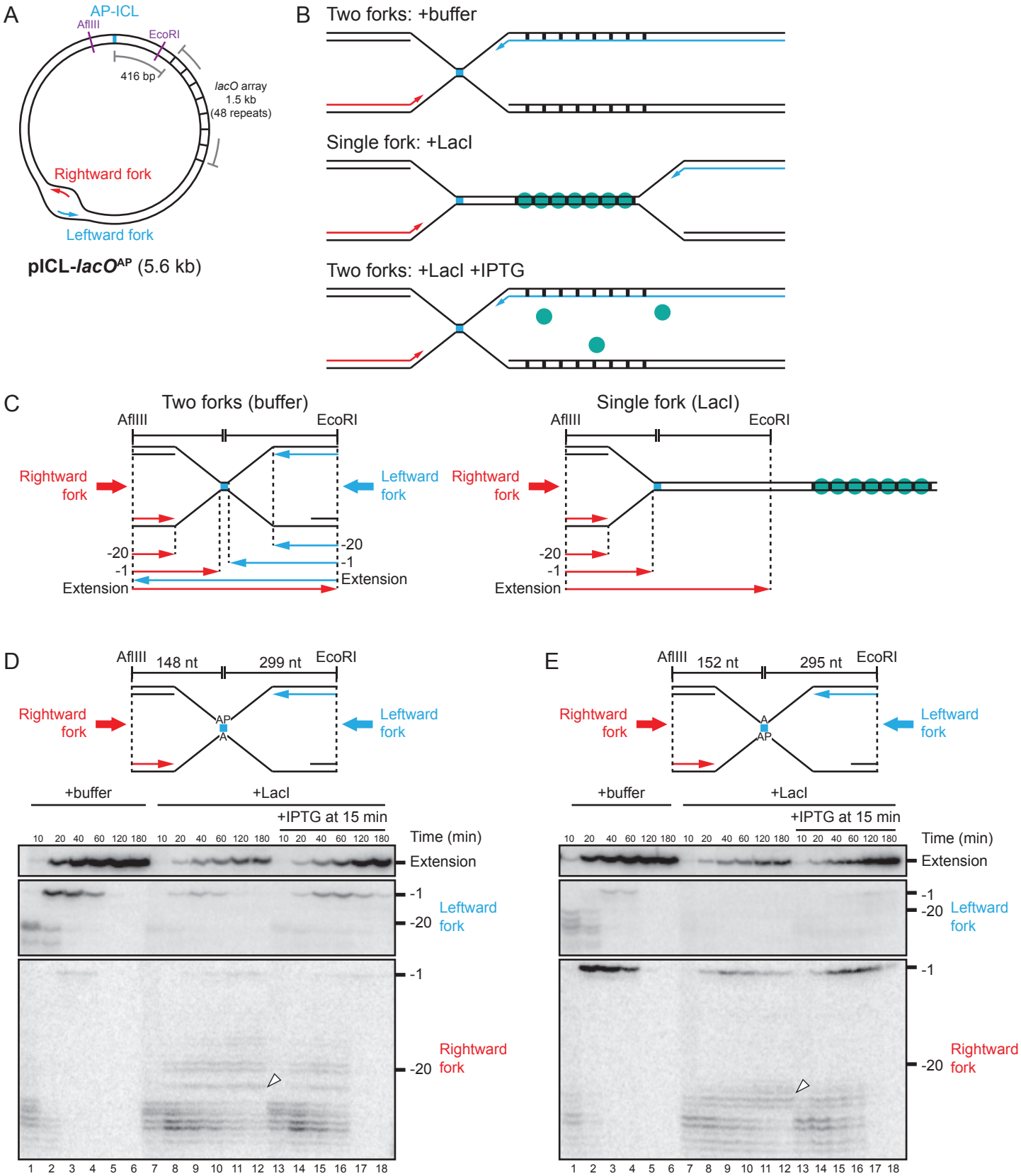

Figure S7